A role for IRF3-dependent RXRα repression in hepatotoxicity associated with viral infections

Edward K. Chow,[1] Antonio Castrillo,[2,3] Arash Shahangian,[4,7] Liming Pei,[2,3] Ryan M. O'Connell,[4] Robert L. Modlin,[4,5] Peter Tontonoz,[2,3] and Genhong Cheng[1,4,6]

[1]Molecular Biology Institute, [2]Howard Hughes Medical Institute, [3]Department of Pathology and Laboratory Medicine, [4]Department of Microbiology, Immunology, and Molecular Genetics, [5]Division of Dermatology, [6]Jonsson Comprehensive Cancer Center, and [7]Medical Scientist Training Program, David Geffen School of Medicine, University of California, Los Angeles, Los Angeles, CA 90095

Viral infections and antiviral responses have been linked to several metabolic diseases, including Reye's syndrome, which is aspirin-induced hepatotoxicity in the context of a viral infection. We identify an interferon regulatory factor 3 (IRF3)–dependent but type I interferon–independent pathway that strongly inhibits the expression of retinoid X receptor α (RXRα) and suppresses the induction of its downstream target genes, including those involved in hepatic detoxification. Activation of IRF3 by viral infection in vivo greatly enhances bile acid– and aspirin-induced hepatotoxicity. Our results provide a critical link between the innate immune response and host metabolism, identifying IRF3-mediated down-regulation of RXRα as a molecular mechanism for pathogen-associated metabolic diseases.

CORRESPONDENCE
Genhong Cheng:
genhongc@microbio.ucla.edu

Abbreviations used: 1,25(OH)$_2$D$_3$, 1α,25-dihydroxyvitamin D3; 9cRA, 9-cis retinoic acid; ALT, alanine aminotransferase; ASA, acetylsalicylic acid; BMM, bone marrow–derived macrophage; FXR, farnesoid X receptor; H&E, hematoxylin and eosin; HDAC1, histone deacetylase 1; IRF, IFN regulatory factor; LCA, lithocholic acid; LXR, liver X receptor; PCN, pregnenolone-16α-carbonitrile; polyI:C, polyinosine-polycytidylic acid; PPAR, peroxisome proliferator–activated receptor; PXR, pregnane X receptor; Q-PCR, quantitative PCR; RXR, retinoid X receptor; TLR, Toll-like receptor; TSA, trichostatin A; UGT1A6, uridine diphosphate glucuronosyltransferase 1A6; USF, upstream stimulatory factor; VDR, vitamin D receptor; VSV, vesicular stomatitis virus.

There is growing evidence that viral infections contribute to the induction or progression of metabolic diseases, potentially through inflammation and other unknown mechanisms. Viral infections have been linked to defects in cholesterol metabolism (1), such as atherosclerosis, and liver metabolism of drugs, as in Reye's syndrome (2), as well as bone metabolism defects, skin eruptions, and diabetes (3–6). There is also evidence that maternal viral infections can lead to the maternal immune system affecting embryonic development, as seen in TORCH infections (7).

A common mechanism in the development of metabolic disorders is the alteration of gene expression controlled by nuclear hormone receptors. Members of this family function as transcriptional regulators of metabolic pathways in multiple cell types. Retinoic X receptors (RXRs) play a uniquely important role in metabolism because of their ability to form heterodimers with many different nuclear receptors, including peroxisome proliferator–activated receptors (PPARs) liver X receptor (LXR), farnesoid X receptor (FXR), vitamin D receptor (VDR), thyroid hormone receptor, pregnane X receptor (PXR), and constitutive androstane receptor (8–17). Thus, any signal that alters RXR function or expression has the potential to affect multiple different metabolic programs. A range of intermediates or end products of metabolic pathways, including bile acids, fatty acids, oxysterols, and steroids, have been shown to regulate gene expression through direct binding to RXR hetrodimeric receptors (11–13, 18–26). Two different RXR heterodimer partners, constitutive androstane receptor and PXR, are activated by xenobiotics and participate in hepatic detoxification pathways. Studies using knockout mice have confirmed that these proteins are essential for proper steroid, drug, and xenobiotic metabolism (18, 23–25, 27). Challenging these mice with xenobiotics or toxic bile acids leads to fatty degeneration, acute liver failure, and death.

Previous work has pointed to the existence of cross talk between nuclear receptor signaling and the innate immune response. Induction of acute phase response by treating mice with LPS has been associated with the down-regulation of certain nuclear receptors in the liver,

The online version of this article contains supplemental material.

including RXR (28–30). Recently, the induction of an antiviral immune response in macrophages has been shown to inhibit LXR/RXR function and cholesterol efflux, suggesting a possible mechanism for viral-induced foam cell formation in atherosclerosis (31). Although the precise mechanisms whereby bacterial or viral infections inhibit nuclear receptor function are unknown, experiments on LXR have implicated IFN regulatory factor 3 (IRF3) (31).

IRF3 is a transcription factor shared by both LPS signaling and the antiviral immune response. Upon viral infection or stimulation with Toll-like receptor (TLR) agonists such as polyinosine-polycytidylic acid (polyI:C) or LPS, IRF3 is phosphorylated by serine/threonine kinases such as TANK-binding kinase 1 or inducible IκB kinase (32). In addition to being activated by TLR-TRIF–dependent pathways (33), intracellular receptors such as retinoic acid–inducible gene I are capable of activating IRF3 upon recognition of polyI:C and RNA viruses (34, 35). After activation, IRF3 promotes transcription of type I IFN genes together with other transcription factors, such as NF-κB and activator protein 1 (32, 36, 37). Although IRF3's role in type I IFN induction is well established, there is emerging data demonstrating that IRF3 also functions as a coactivator of NF-κB in the LPS response (38, 39). Mechanisms whereby IRF3 might function to repress target gene expression, however, have not been elucidated.

In the analysis of non–type I IFN–related roles of IRF3, we have identified a function for this factor in the repression of nuclear receptor–regulated liver metabolism. In this paper, we demonstrate that activation of IRF3 during an antiviral immune response profoundly inhibits hepatic expression of RXRα in vivo. As a consequence of this repression, the expression of multiple nuclear receptor target genes critical for xenobiotic detoxification is compromised. This pathway provides a potential molecular mechanism for the pathogenesis of Reyes' syndrome in which acetylsalicylic
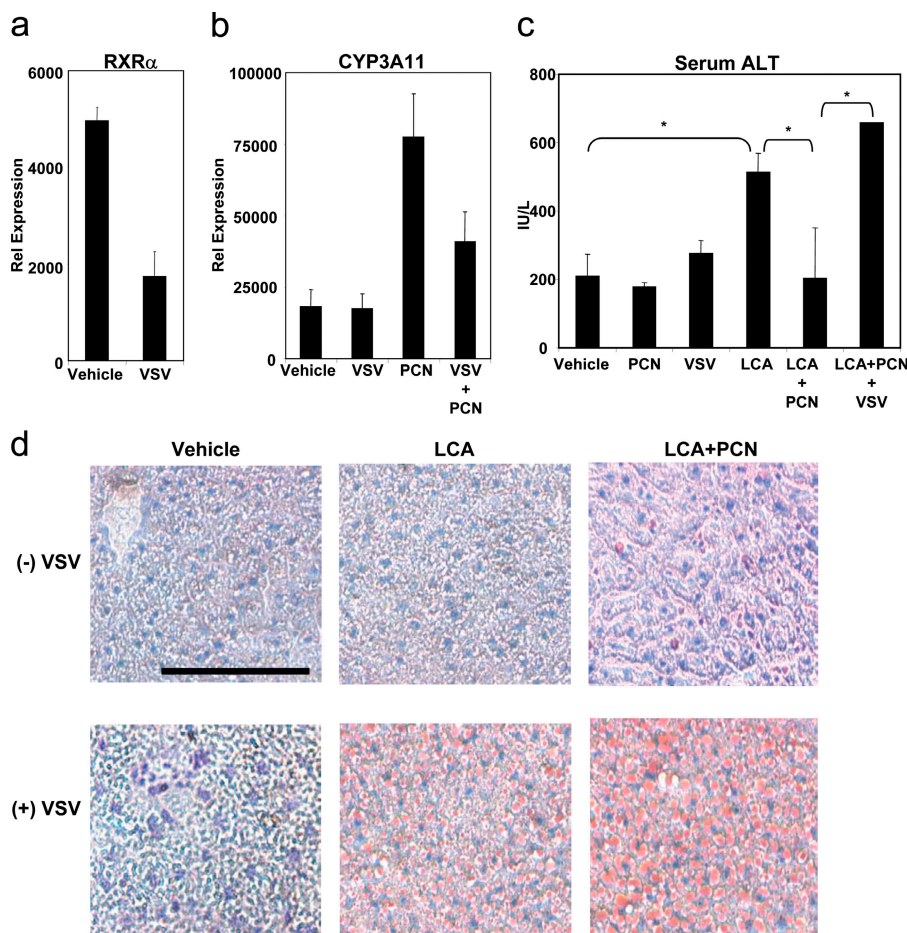

Figure 1. **Viral infections negatively regulate in vivo RXR het–erodimer target genes and liver metabolism.** (a and b) Wild-type mice ($n = 4$) were treated with 0.1% NaCl or 2.5×10^7 PFU VSV i.v. on day 1 with or without vehicle (1% DMSO, maize oil) and 75 mg/kg PCN by gavage for 4 d. Liver RNA was analyzed by Q-PCR. Error bars represent mean ± SD. (c) Wild-type mice ($n = 4$) were treated with 0.1% NaCl or 2.5×10^7 PFU VSV i.v. on days 1 and 3, as well as vehicle (1% DMSO, maize oil) and 75 mg/kg PCN by gavage and/or 0.25 mg/kg LCA i.p. for 4 d. Serum was collected and analyzed for serum ALT as described in Materials and methods. Error bars represent mean ± SD. *, P ≤ 0.001. (d) Representative oil red O staining of livers isolated after treatment in c. Bar, 50 μm.

acid (ASA; i.e., aspirin) treatment during a viral infection leads to hepatotoxicity. Repression of RXRα expression and downstream target genes by IRF3 may represent a critical mechanism underlying metabolic diseases associated with viral infections.

RESULTS
Antiviral immune response represses RXRα and liver metabolism in vivo

To investigate the relationship between liver metabolism and viral infections, C57/Bl6 mice were infected with vesicular stomatitis virus (VSV), and nuclear receptor function was analyzed. VSV infection potently down-regulated expression of *RXRα* mRNA in vivo (Fig. 1 a). Furthermore, down-regulation of this critical heterodimeric partner for hepatic nuclear receptors was associated with the inhibition of multiple nuclear receptor pathways, including induction of PXR-mediated *CYP3A11* by pregnenolone-16α-carbonitrile (PCN) and VDR-mediated induction of *CYP24* mRNA by 1α,25-dihydroxyvitamin D3 (1,25(OH)$_2$D$_3$; Fig. 1 b and Fig. S1, available at http://www.jem.org/cgi/content/full/jem.20060929/DC1). Furthermore, VSV infections in the Huh7 hepatocyte cell line resulted in inhibition of hepatic LXR, FXR, and PPARα-mediated induction of hepatic nuclear receptor target genes (Fig. S1).

Detoxification and clearance of secondary bile acids, such as lithocholic acid (LCA), is an important metabolic function of the liver required for physiologic homeostasis. Defective metabolism of LCA or excessive amounts of LCA results in cholestasis and hepatotoxicity. PCN activation of PXR/RXR has been previously shown to protect the liver from secondary bile acid (LCA)–induced hepatotoxicity through induction of *CYP3A11* and other genes involved in the metabolism of LCA (18, 27). In wild-type mice, administration of LCA in excess of natural levels led to significant elevation of serum alanine aminotransferase (ALT) levels, which was reduced by cotreatment with PCN (Fig. 1 c). To determine the impact of viral infection on nuclear receptor–regulated bile acid metabolism, the LCA cholestasis model was analyzed in the context of VSV infection. Although VSV infection alone had no effect on serum ALT levels, it blocked the ability of PCN to reduce LCA-induced serum ALT levels (Fig. 1 c). Furthermore, VSV infection induced fatty change and hepatotoxicity in LCA-treated mice, as demonstrated by oil red O staining (Fig. 1 d). The VSV plus LCA–induced hepatotoxicity could not be blocked by the addition of PCN. Thus, viral infections inhibit PXR/RXR-dependent gene expression and promote LCA-induced liver damage.

To determine the mechanism responsible for the inhibition of hepatic gene expression and metabolism observed during viral infection, experiments were repeated with polyI:C, representing viral dsRNA. Treatment with polyI:C resulted in a substantial reduction in *RXRα* mRNA expression (Fig. 2 a). Additionally, polyI:C blunted the induction of *CYP3A11* by PCN as well as the induction of *CYP24* by the VDR agonist 1,25(OH)$_2$D$_3$ (Fig. 2 a and Fig. S1). Furthermore,

hepatic LXR, FXR, and PPARα target genes were also inhibited by polyI:C treatment in Huh7 cells (Fig. S1). Both polyI:C and viruses such as VSV are known to activate IRF3, a key mediator of the antiviral immune response. Experiments with IRF3 knockout mice established that IRF3 was critical for the repression of *RXRα* and hepatic nuclear receptor target genes by polyI:C (Fig. 2 a and Fig. S1). Furthermore, addition of the nuclear receptor agonist PCN to polyI:C treatment resulted in a further loss of RXRα protein expression (Fig. 2 b).

Similar to the results obtained with VSV, treatment of mice with polyI:C alone did not significantly increase serum ALT levels. However, polyI:C in combination with LCA strongly induced liver damage, and this damage was not blocked by PCN (Fig. 2, c and d). Moreover, polyI:C failed to promote LCA-mediated increases of serum ALT levels or enhance liver damage in IRF3$^{-/-}$ mice, demonstrating the requirement for IRF3 in polyI:C regulation of hepatic gene expression and function. (Fig. 2, c and d). These experiments establish that viral activation of IRF3 inhibits hepatic nuclear receptor target gene induction and metabolic activity, resulting in potentiation of LCA-mediated hepatotoxicity.

PolyI:C and LPS repress RXRα expression through IRF3

To gain a greater understanding of the molecular mechanisms behind innate immune system repression of RXRα and RXRα target genes, we confirmed, by quantitative PCR (Q-PCR), that polyI:C and LPS repressed *RXRα* mRNA in bone marrow–derived macrophages (BMMs) after 4 h of stimulation (Fig. 3 a). Furthermore, an extended time course indicated that polyI:C is a more potent repressor of *RXRα* mRNA than LPS (Fig. 3 b). These data validate the in vitro model as representative of our in vivo studies, because *RXRα* mRNA expression is inhibited by viral infections and TLR ligands in both systems. Protein expression analysis revealed that RXRα protein loss after polyI:C treatment was more obvious upon the addition of RXR-specific (LG268, LG) or LXR-specific (GW3965, GW3) agonists (Fig. 3 d). Previously, IRF3 was found to be involved in the repression of LXR target genes in BMMs (31). Because RXRα cell type–specific knockout studies have demonstrated critical roles for RXRα target genes (19, 26, 40, 41), we examined the mechanism for such repression in greater detail.

Next, we explored the mechanism of RXRα repression by analyzing the contribution of IRF3 and type I IFNs, as these are the main signaling mediators shared by TLR3 and TLR4 but not TLR9 in macrophages. PolyI:C-mediated inhibition of *RXRα* was defective in IRF3$^{-/-}$ BMMs but not IFNAR$^{-/-}$ BMMs (Fig. 3 c). Similar regulation was seen at the protein level, as RXRα protein expression levels were considerably higher in IRF3$^{-/-}$ compared with IFNAR$^{-/-}$ BMMs (Fig. 3 e). Although there was some loss of RXRα protein in IRF3$^{-/-}$ BMMs after polyI:C and LG268 treatment, the protein levels were substantially higher than in wild-type or IFNAR$^{-/-}$ BMMs, whereas upstream stimulatory factor 2 (USF2) levels were equivalent. These data
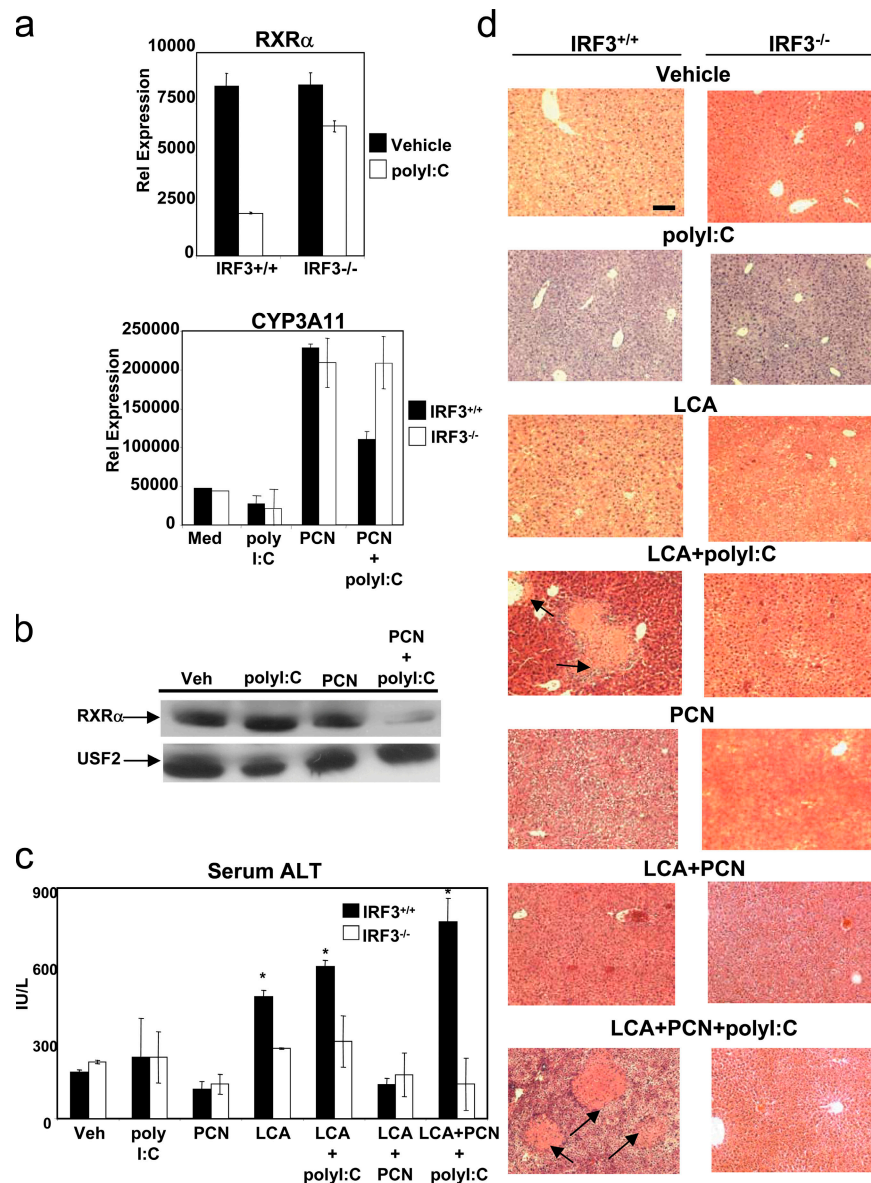
Figure 2.   PolyI:C negatively regulated in vivo RXR heterodimer tar-get genes and liver metabolism. (a) Wild-type or IRF3$^{-/-}$ mice ($n = 4$) were treated with 0.1% NaCl or 150 μg polyI:C i.v. on days 1 and 3 with or without vehicle (1% DMSO, maize oil) or 75 mg/kg PCN by gavage for 4 d. Liver RNA were analyzed by Q-PCR. Error bars represent represent mean ± SD. (b) Representative anti-RXRα and anti-USF2 Western blots of wild-type livers after treatment with 0.1% NaCl or 150 μg polyI:C i.v. on days 1 and 3 with or without vehicle or 75 mg/kg PCN by gavage for 4 d. (c) Wild-type or IRF3$^{-/-}$ mice ($n = 4$) were treated with 0.1% NaCl or 150 μg polyI:C i.v. on days 1 and 3, as well as vehicle (1% DMSO, maize oil) and 75 mg/kg PCN by gavage and/or 0.25 mg/kg LCA i.p. for 4 d. Serum was collected and ana-lyzed for serum ALT as described in Materials and methods. Error bars rep-resent mean ± SD. *, P ≤ 0.001. (d) Representative H&E staining of livers isolated after treatment in c. Arrows indicate necrotic foci. Bar, 100 μm.

suggest the existence of an IRF3-dependent, type I IFN–in-dependent pathway for RXRα repression.

Optimal transcription of nuclear receptor target genes is known to require degradation of nuclear receptors, such as RXRα, by the 26S proteosome complex (42). New pro-tein synthesis replaces degraded nuclear receptors on the promoters of these target genes during transcription (42). We analyzed whether nuclear receptor activation of the 26S proteosome complex would coordinate with IRF3-mediated

inhibition of *RXRα* mRNA expression to contribute to the loss of RXRα protein. Indeed, MG132, a 26S proteosome complex inhibitor, prevented loss of RXRα protein after co-stimulation with the RAR/RXR agonist 9-cis retinoic acid (9cRA) and polyI:C in BMMs (Fig. 3 f). Thus, maximal RXRα protein loss likely requires combinatorial repres-sion of *RXRα* mRNA by polyI:C and activation of 26S proteosome complex–mediated degradation by nuclear receptor agonists.
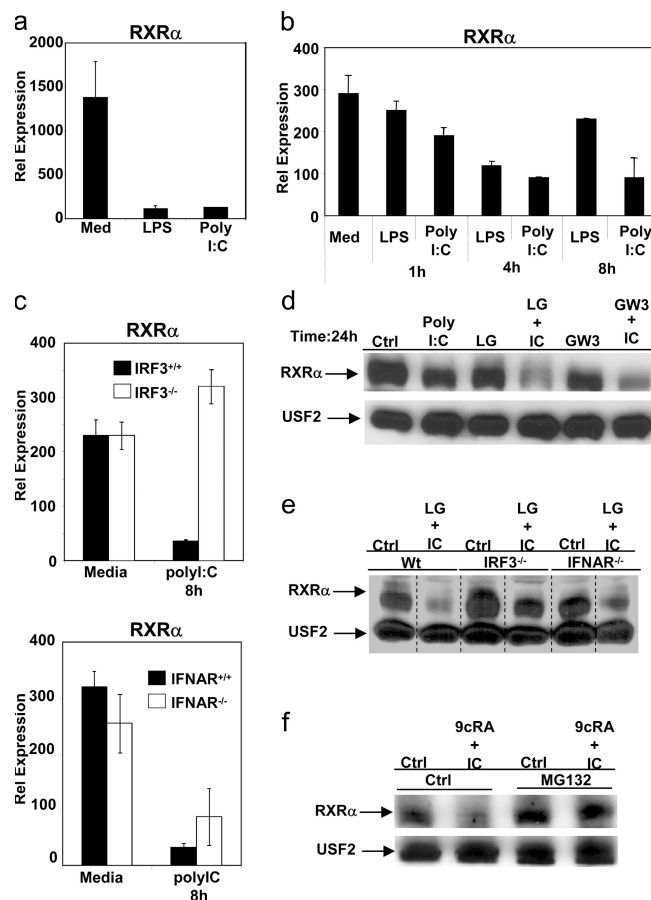
Figure 3. RXRα repression by polyI:C/LPS requires IRF3 but not type 1 IFNs. (a) BMMs were stimulated with 10 ng/ml LPS or 1 μg/ml polyI:C for 4 h. RNA was collected and analyzed by Q-PCR. (b) BMMs were stimulated with 10 ng/ml LPS or 1 μg/ml polyI:C for 1, 4, or 8 h. RNA was analyzed by Q-PCR. (c) Wild-type, IRF3$^{-/-}$, and IFNAR$^{-/-}$ BMMs and their wild-type controls were stimulated with 1 μg/ml polyI:C for 8 h. RNA was analyzed by Q-PCR. Error bars in a–c represent mean ± SD. (d) BMMs were stimulated with control (DMSO), 10 nM LG268, and 1 μM GW3965 with or without 1 μg/ml polyI:C for 24 h. Anti-RXRα and anti-USF2 Western blot analysis was done with 75 μg of whole cell extract. (e) Wild-type, IRF3$^{-/-}$, and IFNAR$^{-/-}$ BMMs were stimulated with control (DMSO), 10 nM LG268, and 1 μg/ml polyI:C for 24 h. Anti-RXRα and anti-USF2 Western blot analysis was done with 75 μg of whole cell extract. (f) BMMs were stimulated with control (DMSO) or 10 μM MG132 with or without control (DMSO) or 9cRA and polyI:C. Anti-RXRα and anti-USF2 Western blot analysis was done with 75 μg of whole cell extract.

IRF3 inhibits RXRα transcription through induction of the transcriptional suppressor Hes1

We further analyzed potential transcriptional and posttranscriptional mechanisms through which polyI:C might repress *RXRα*. BMMs were pretreated with or without polyI:C for 2 h and treated with actinomycin D (a transcription inhibitor) to measure *RXRα* mRNA stability. No important differences were observed in *RXRα* mRNA stability from samples treated with or without polyI:C, suggesting that repression is not posttranscriptionally regulated (Fig. 4 a).

Furthermore, *RXRα* primary transcripts measured by Q-PCR using primers that amplify a region spanning an exon and intron were strongly repressed after polyI:C treatment (Fig. 4 a). Collectively, these data indicate that polyI:C regulates *RXRα* expression at the level of transcription.

To gain greater insight into how *RXRα* is transcriptionally repressed by polyI:C, the promoter region of *RXRα* (from −1 to −1,000 bp) was analyzed for predicted transcription factor binding sites. Using promoter analysis software (see legend to Fig. 4), highly predicted binding sites were identified by core similarity (>0.9) and matrix similarity (>0.9). The first 400 bp of the promoter identified multiple hits for three known transcriptional repressors: Hes1, ZF5, and ZNF202 (Fig. 4 b). Hes1 and ZNF202 have previously been identified as potential transcriptional regulators of cholesterol metabolism (43, 44). *Hes1* mRNA was potently induced by polyI:C and LPS (Fig. 4 b), whereas ZF5 and ZNF202 mRNA levels were unaffected (not depicted). Although it is known that NF-κB activators like TNF-α can induce *Hes1* (45), our data indicate that polyI:C induction of *Hes1* also involves IRF3 but not type I IFNs (Fig. 4 b). Preliminary *Hes1* promoter analysis indicates an IFN-stimulated regulatory element (−722/−751) with core similarity of 1 and matrix similarity of 0.91 (unpublished data), but further studies are required to determine if direct binding of IRF3 to the *Hes1* promoter is involved in the polyI:C-induced *Hes1* up-regulation.

To assess the ability of Hes1 to repress *RXRα* and RXR-related genes, RAW 264.7 cells stably transfected with pCMV-Hes1 were compared with empty vector controls in terms of *RXRα* mRNA expression and function. Fig. 4 c shows that overexpression of Hes1 led to the specific down-regulation of *RXRα* mRNA, with control *L32* mRNA being unaffected. Furthermore, knockdown experiments with siRNA specific to Hes1 demonstrated the requirement of Hes1 in polyI:C-mediated repression of RXRα (Fig. 4 d).

Hes1 mediates gene repression by recruiting the Gro/TLE tetramer and histone deacetylase 1 (HDAC1) complex to the promoter region of its target genes (46). Chromatin immunoprecipitation of Hes1 and HDAC1 demonstrated that polyI:C promotes specific recruitment of Hes1 and HDAC1 to the *RXRα* promoter region and predicted Hes1 binding site (Fig. 4, e and f). To test if recruitment of Hes1 and HDAC1 is involved in polyI:C repression of *RXRα*, BMMs were pretreated with or without the HDAC1 inhibitor, trichostatin A (TSA), followed by stimulation with polyI:C. The addition of TSA prevented polyI:C repression of *RXRα* and allowed polyI:C to induce *RXRα* (Fig. 4 g), providing further evidence for a novel mechanism of repression of RXRα by polyI:C.

Transcriptional repression of *RXRα* results in defective induction of RXR target genes

We predicted that the expression of RXRα target genes would mirror regulation of RXRα by polyI:C. Indeed, just as polyI:C induced down-regulation of *RXRα* requires IRF3
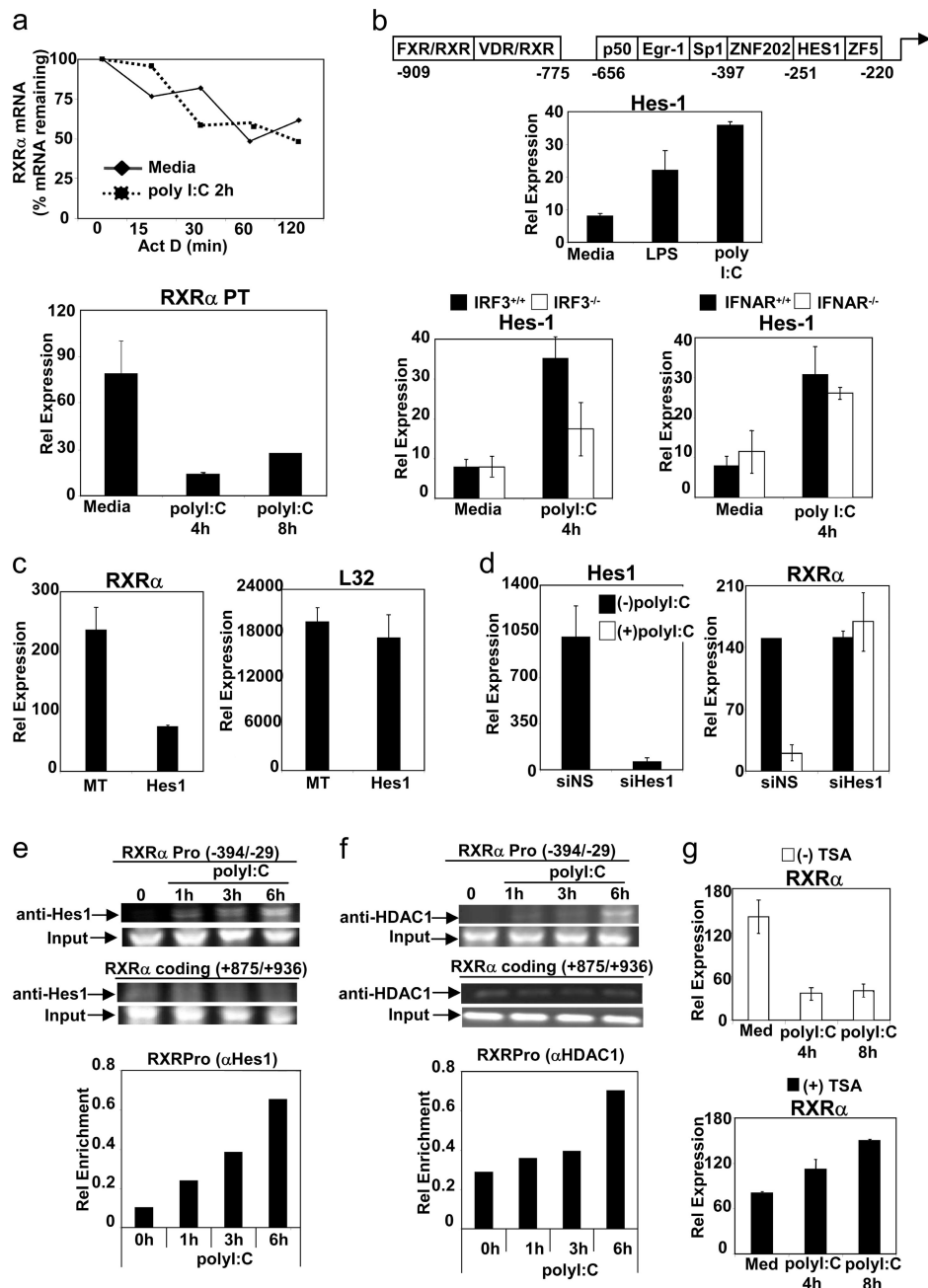
Figure 4.   Polyl:C transcriptionally represses *RXRα* through recruitment of transcriptional repression machinery. (a) BMMs were stimulated with media or 1 μg/ml polyl:C for 2 h, followed by 5 μg/ml actinomycin D (Act D) for 0, 15, 30, 60, and 120 min. BMMs were stimulated with 1 μg/ml polyl:C for 4 or 8 h. RNA was analyzed by Q-PCR. (b) Diagram of the RXRα promoter based on promoter analysis software (MatInspector; www.genomatix.de). BMMs were stimulated with 10 ng/ml LPS or 1 μg/ml polyl:C for 4 h. RNA was analyzed by Q-PCR. Wild-type, IRF3$^{-/-}$, and IFNAR$^{-/-}$ BMMs were stimulated with 1 μg/ml polyl:C for 4 h. RNA was analyzed by Q-PCR. (c) pCMV–RAW 264.7 cells (MT) or pCMV–Hes1–RAW 264.7 cells (Hes1). RNA was analyzed by Q-PCR. (d) RAW264.7 cells transfected with siNS or siHes1 duplex oligos were stimulated with 1 μg/ml polyl:C for 8 h. RNA was analyzed by Q-PCR. Error bars in a–d represent mean ± SD. (e and f) BMMs were stimulated with 1 μg/ml polyl:C for 1, 3, and 6 h. After stimulation, chromatin immunoprecipitation was performed with anti-Hes1 or anti-HDAC1 antibodies on sonicated samples, washed thoroughly, and analyzed by PCR/agarose gel electrophoresis. PCR products on gel are quantified by ImageJ, normalized to input. (g) BMMs were pretreated with 50 ng/ml TSA overnight and stimulated with 1 μg/ml polyl:C for 4 and 8 h. RNA was analyzed by Q-PCR. Error bars represent mean ± SD.

and is independent of type I IFNs, induction of the RXRα target gene *CRBPII* by synthetic RXR ligand (LG268) was repressed by polyl:C in IFNAR$^{-/-}$ BMMs but not IRF3$^{-/-}$

BMMs (Fig. 5 a). Because repression of RXRα by polyl:C appears to require Hes1, we analyzed the role of Hes1 in repression of RXRα target genes. As seen in Fig. 5 b,

overexpression of Hes1 in RAW 264.7 cells prevents the RAR/RXR agonist, 9cRA, from inducing *CRBPII* and *ABCA1*. Furthermore, polyI:C is unable to repress 9cRA induction of *CRBPII* in cells with knockdown of Hes1 (Fig. 5 c).

To determine if loss of RXRα contributes to polyI:C repression of nuclear receptor–regulated genes, we analyzed RAW 264.7 cells stably expressing RXRα (Fig. S2, available at http://www.jem.org/cgi/content/full/jem.20060929/DC1). PolyI:C was unable to repress LG268-induced *CRBPII* in the RXRα-overexpressing RAW 264.7cells (Fig. 5 d). Additionally, we examined whether repression of RXRα is a key requirement of polyI:C repression of RXRα target hepatic genes. As seen in Fig. 5 e, transfected polyI:C was capable of repressing rifampicin induction of the human homologue to *CYP3A11*, *CYP3A4*, in Huh7 cells, a human hepatocyte cell line. In the presence of RXRα overexpression (Fig. S2), however, polyI:C no longer repressed *CYP3A4* (Fig. 5 e). These results were matched in the induction of another RXR-regulated gene, *uridine diphosphate glucuronosyltransferase 1A6* (*UGT1A6*), which is induced by and metabolizes ASA (Fig. 5 f) (47, 48).

Finally, we also confirmed by chromatin immunoprecipitation that transcriptional repression of RXRα results in a reduction of RXRα present on the promoter of RXRα target hepatic gene, *CYP3A4*. As shown in Fig. 5 (g and h), combinatorial treatment of Huh7 cells with rifampicin and polyI:C resulted in maximal loss of RXRα in the PXR/RXR ER6 binding region of *CYP3A4*, whereas binding was minimal and unchanged in the upstream coding region. These data present evidence that IRF3-mediated transcriptional repression of *RXRα* by transfected and nontransfected polyI:C is integral to the repression of RXR-related target genes.

Viral infection greatly enhanced ASA hepatotoxicity, a potential mouse model of Reye's syndrome

Based on our in vivo and in vitro results, we hypothesized that metabolic disorders involving both nuclear receptor–regulated xenobiotic metabolism and viral infections might involve the repression of RXR target genes by IRF3 during host immune response. A human disease that involves viral infection and metabolic hepatotoxicity is Reye's syndrome, characteristically presenting with delirium and fatty degeneration of the liver in a child with a history of an antecedent viral infection treated with ASA. We speculated that the pathogenesis of Reye's syndrome might be caused, at least in part, by this mechanism of antiviral immune response and nuclear receptor cross talk and subsequent metabolic dysfunction. To test this hypothesis, we analyzed the effects of ASA treatment in the presence and absence of an antiviral immune response initiated by polyI:C or VSV. Treatment of mice with ASA, polyI:C, or VSV alone did not cause substantial hepatotoxicity. Administration of ASA to mice treated with polyI:C or infected with VSV, however, caused severe hepatotoxicity, as indicated by liver necrosis or fatty degeneration (Fig. 6, a and d). Consistent with a Reye's syndrome–like phenotype, serum ALT, ammonia, and total bilirubin levels were increased

during coadministration of ASA and polyI:C or VSV, whereas blood glucose levels were significantly decreased (Fig. 6, b, c, and e–g) (49–51). Interestingly, hepatotoxicity from exposure to polyI:C plus ASA did not occur in IRF3$^{-/-}$ mice, but did occur in IFNAR$^{-/-}$ mice (Fig. 6, d–f). It has been previously shown that polyI:C treatment results in defective ASA metabolism, possibly contributing to the hepatotoxicity seen in our experiment (52). In addition to CYP3A4 (53, 54), another enzyme that is induced by ASA and involved in the metabolism of ASA is UGT1A6, whose gene is also regulated by PXR/RXR (48). UGT1A6 glucoronidates the ASA intermediate, salicylic acid (55), and defects in UGT1A6 have been associated with impaired metabolism of aspirin (47). Interestingly, treatment with ASA or the PXR/RXR agonist PCN potently increased *UGT1A6* and *CYP3A11* mRNA in vivo, but not other PXR/RXR genes such as *Oatp2* that are likely not involved in ASA metabolism (Fig. 1 b; Fig. 2 a; Fig. 7, a and b; and Fig. S3, available at http://www.jem. org/cgi/content/full/jem.20060929/DC1). Furthermore, this induction was diminished by either polyI:C stimulation or VSV infection (Fig. 1 b; Fig. 2 a; Fig. 7, a and b; and Fig. S3). Additionally, the repression of *UGT1A6* by polyI:C was dependent on IRF3 (Fig. S3). The biological loss of RXRα likely contributes to this effect. Just as the loss of RXRα decreases *CYP3A11* expression in mice or *CYP3A4* in Huh7 cells (Fig. 7 e) (23), *UGT1A6* induction by ASA is impaired in Huh7 cells that have RXRα silenced by siRNA (Fig. 7 e), and ASA and polyI:C cotreatment resulted in a considerable loss of RXRα protein, just as PCN and polyI:C treatment led to the potent loss of RXRα protein (Fig. 7 d).

Mechanisms for ASA toxicity are likely through membrane permeability transition and mitochondrial injury, which is caused by ASA's intermediate, salicylic acid, destabilization of mitochondrial calcium homeostasis (56). Rhodamine 123 assays demonstrate that RXRα repression by polyI:C results in loss of mitochondrial membrane potential in mock-transfected Huh7 cells cotreated with ASA and polyI:C but not in Huh7 cells overexpressing RXRα (Fig. S4, available at http://www.jem.org/cgi/content/full/jem.20060929/DC1). These in vivo and in vitro observations provide evidence that cross talk between antiviral immune responses and nuclear receptor signaling may play a critical role in the pathogenesis of Reye's syndrome.

DISCUSSION

The connection between viral infections and metabolic dysfunction is an important clinical problem, yet the mechanisms linking these events are not understood. In this paper we provide in vivo evidence for a novel pathway linking viral infection to metabolic disease. We have shown that activation of IRF3 during the viral immune response leads to a profound suppression of RXRα mRNA and protein expression. Because RXRα serves as an obligatory heterodimeric partner for several nuclear receptors involved in metabolic control, these observations provide a molecular explanation for how viral infections can alter a range of metabolic pathways.
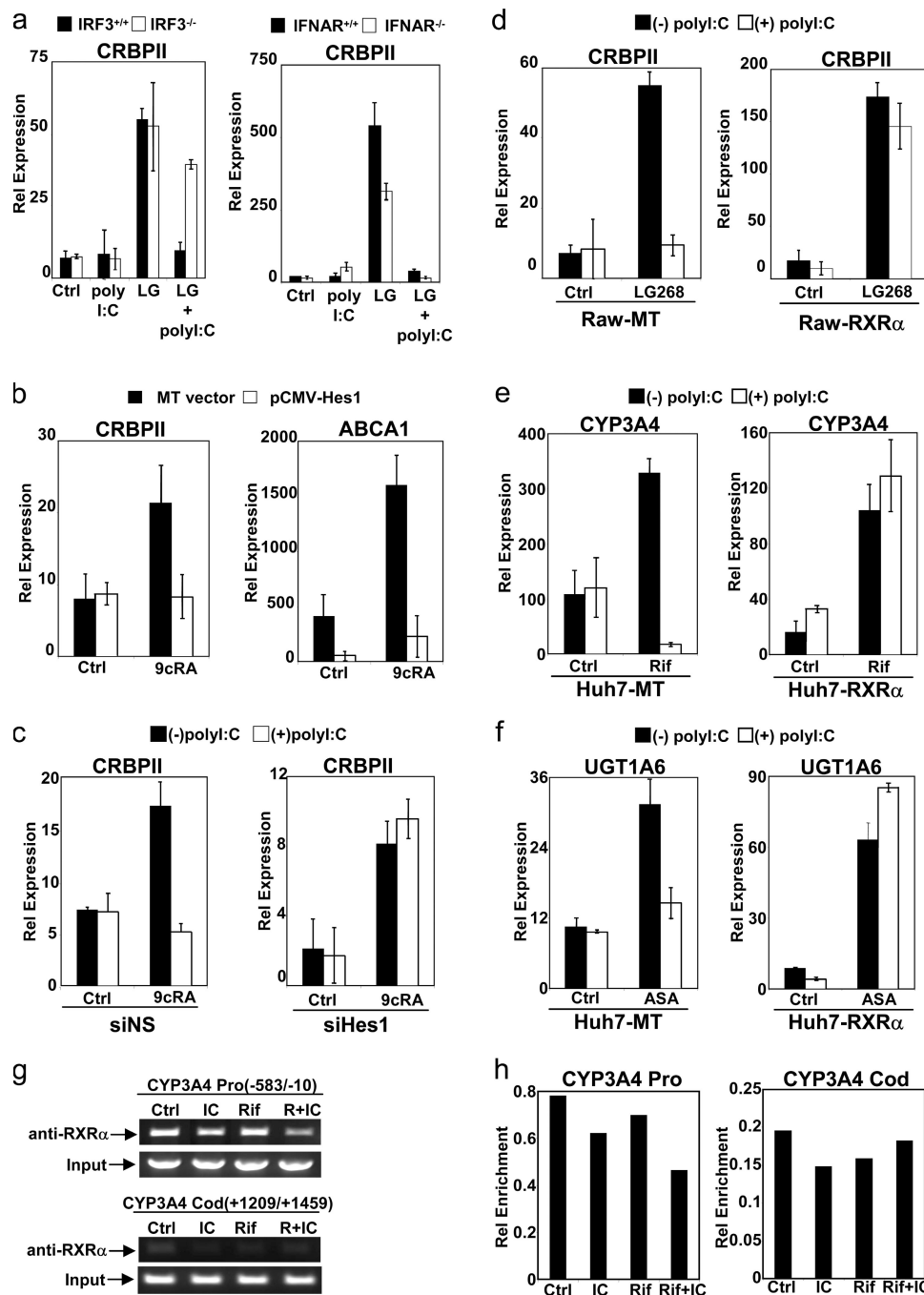
Figure 5. PolyI:C transcriptional repression of *RXRα* is critical for repression of nuclear receptor target genes. (a) Wild-type, IRF3$^{-/-}$, and IFNAR$^{-/-}$ BMMs were stimulated with control (DMSO) or 10 nM LG268 with or without 1 μg/ml polyI:C. RNA was analyzed by Q-PCR. (b) pCMV–RAW 264.7 cells (MT) or pCMV–Hes1–RAW 264.7 cells (Hes1) were stimulated with control (DMSO) and 9cRA with or without 1 μg/ml polyI:C for 24 h. RNA was analyzed by Q-PCR. (c) RAW 264.7 cells transfected with siNS or siHes1 duplex oligos were stimulated with control (DMSO) and 10 μM 9cRA with or without 1 μg/ml polyI:C for 24 h. RNA was analyzed by Q-PCR. (d) pBabe–RAW 264.7 cells (RAW-MT) and pBabe-RXRα–RAW264.7 cells (RAW-RXRα) were stimulated with control (DMSO) or 10 nM LG268 with or without 1 μg/ml polyI:C for 24 h.

RNA was analyzed by Q-PCR. (e) pBabe-Huh7 cells (Huh7-MT) and pBabe-RXRα-Huh7 cells (Huh7-RXRα) were stimulated with control (DMSO) and 25 μM rifampicin with or without 2 μg/ml polyI:C (transfected). RNA was analyzed by Q-PCR. (f) pBabe-Huh7 cells (Huh7-MT) and pBabe-RXRα-Huh7 cells (Huh7-RXRα) were stimulated with control (DMSO) and 20 μg/ml ASA with or without 2 μg/ml polyI:C (transfected). RNA was analyzed by Q-PCR. Error bars in a–f represent mean ± SD. (g and h) BMMs were stimulated with 25 μM rifampicin and 1 μg/ml polyI:C for 24 h. After stimulation, chromatin immunoprecipitation was performed with anti-RXRα antibody on sonicated samples, washed thoroughly, and analyzed by PCR/agarose gel electrophoresis. PCR products on gel are quantified by ImageJ, normalized to input. Error bars represent mean ± SD.
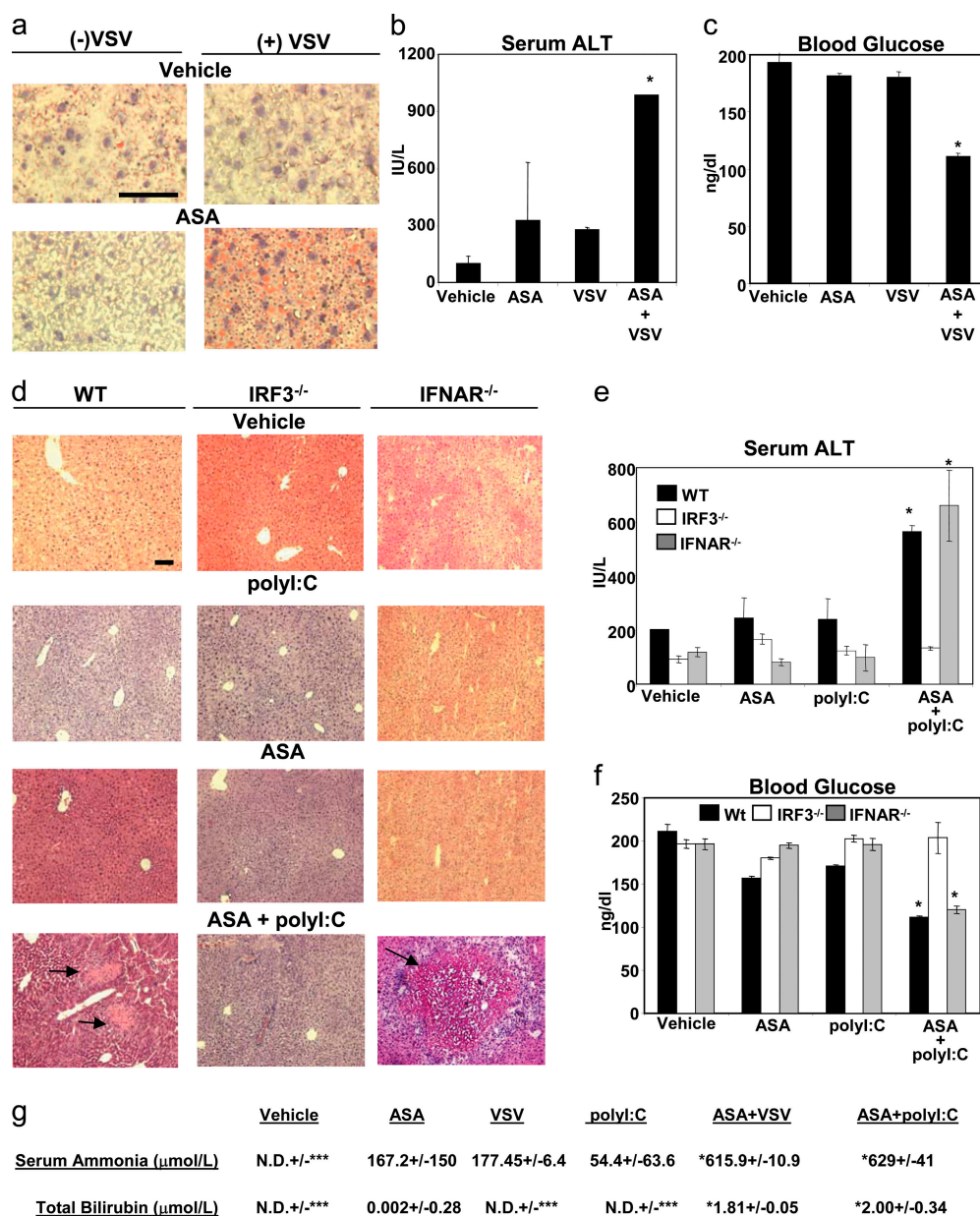
Figure 6. **PolyI:C and viral infection promote ASA–related hepato-toxicity through IRF3, independent of type I IFNs.** (a) Representative oil red O staining of livers from wild-type mice (*n* = 4) treated with 0.1% NaCl or 2.5 × 10⁷ PFU VSV i.v. on day 1 with or without 3.25 g/L ASA in drinking water for 4 d. Bar, 50 μm. (b and c) Wild-type mice (*n* = 4) were treated with 0.1% NaCl or 2.5 × 10⁷ PFU VSV i.v. on day 1 with or without 325 mg/L ASA in drinking water for 4 d. Serum was collected, and serum ALT and blood glucose were analyzed as described in Materials and meth-ods. Error bars represent mean ± SD. *, P ≤ 0.001. (d) Representative H&E staining of livers from wild-type, IRF3⁻/⁻, and IFNAR⁻/⁻ mice treated with 0.1% NaCl or 150 μg poly I:C i.v. on days 1 and 3 with or without 3.25 g/L ASA in drinking water for 4 d. Arrows indicate necrotic foci. Bar, 100 μm. (e and f) Wild-type, IRF3⁻/⁻, or IFNAR⁻/⁻ mice (*n* = 4) were treated with 0.1% NaCl or 150 μg polyI:C i.v. on days 1 and 3 with or without 3.25 g/L ASA in drinking water for 4 d. Serum was collected, and serum ALT and blood glucose were analyzed as described in Materials and methods. Error bars represent mean ± SD. *, P ≤ 0.001. (g) Wild-type mice (*n* = 4) were treated with 0.1% NaCl or 2.5 × 10⁷ PFU VSV i.v. on day 1 or 150 μg polyI:C i.v. on days 1 and 3 with or without 3.25 g/L ASA in drinking water for 4 d. Serum was collected, and serum ammonia and total bilirubin levels were analyzed as described in Materials and methods. *, P ≤ 0.01.

As a consequence of RXRα suppression during viral infec-tion, the expression of multiple downstream nuclear receptor target genes is compromised, including those required for liver detoxification of endogenous and exogenous com-pounds and those required for lipid metabolism. Moreover, the ability of viral infections to repress nuclear receptor func-tion leads to hepatotoxicity in the context of endogenous toxins such as LCA and exogenous compounds such as ASA.
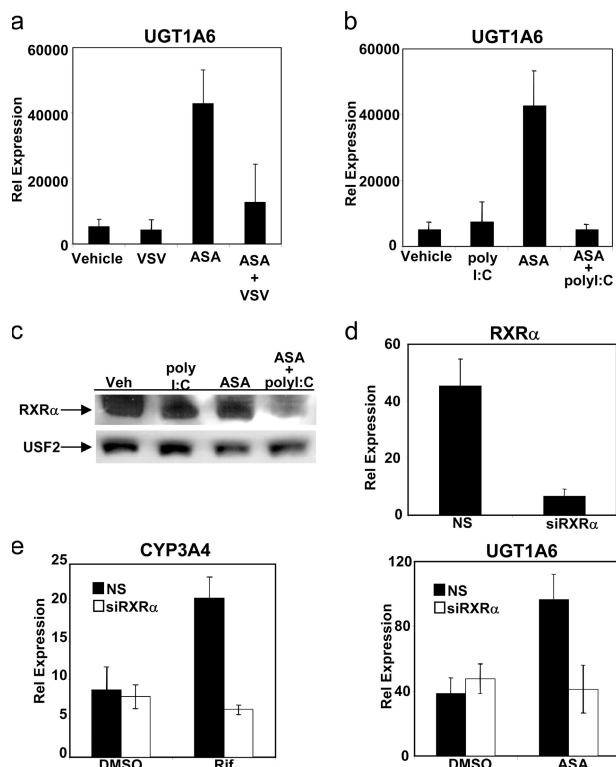
Figure 7. PolyI:C and viral infection inhibit ASA induction of UGT1A6. (a) Wild-type mice ($n = 4$) were treated with 0.1% NaCl or 2.5×10^7 PFU VSV i.v. on day 1 with or without 3.25 g/L ASA in drinking water for 4 d. Liver samples were isolated, and RNA was analyzed by Q-PCR. (b) Wild-type mice ($n = 4$) were treated with 0.1% NaCl or 150 μg polyI:C i.v. on days 1 and 3 with or without 3.25 g/L ASA in drinking water for 4 d. Liver samples were isolated, and RNA was analyzed by Q-PCR. Error bars in a and b represent mean $\pm$ SD. (c) Representative Western blot of RXRα and USF2 from samples in b. (d and e) Huh7 cells transfected with siNS or siRXRα duplex oligos were stimulated with 25 μM rifampicin or 20 μg/ml ASA for 24 h. RNA was analyzed by Q-PCR. Error bars represent mean $\pm$ SD.

These data provide a molecular mechanism to explain how viral infections may interfere with liver homeostasis and contribute to the pathogenesis of metabolic disease (Fig. 8).

The clinical relevance of IRF3-mediated inhibition of liver metabolism is illustrated by its potential role in the pathogenesis of hepatic metabolic disorders that involve xenobiotics (drugs and chemicals) ingested during viral infections. One such disorder, Reye's syndrome, has yet to be explained mechanistically. It is known that ASA therapy during a viral infection in children can lead to fatty degeneration of the liver and encephalopathy (2). Not specific to any virus in particular, Reye's syndrome is associated with chickenpox, influenza A or B, adenoviruses, hepatitis A viruses, paramyxovirus, picornaviruses, reoviruses, herpesviruses, measles, and varicella–zoster viruses (49, 57–62). Previous experiments have suggested that hepatotoxicity in Reye's syndrome results from a toxic combination of ASA metabolites and inflammatory cytokines generated in response to a viral infection

(63). It has also been shown that polyI:C can inhibit the metabolism of aspirin, and this has been suggested to occur through type I IFNs (52). Our experimental model of polyI:C/VSV and ASA treatment, however, clearly demonstrates that hepatotoxicity and fatty degeneration occurs in an IRF3-dependent, type I IFN–independent manner, consistent with those seen during Reye's syndrome. Furthermore, it appears that this pathogenesis arises from IRF3 repression of RXRα and its hepatic target genes involved in ASA metabolism. We showed that this repression of RXRα blocks ASA and PCN induction of *UGT1A6* and *CYP3A11*, RXR heterodimer target genes involved in ASA metabolism, and results in increased mitochondrial damage by ASA, a known contributing factor to the pathogenesis of Reye's syndrome (56, 64–66). Our results therefore provide compelling evidence for the involvement of IRF3–nuclear receptor cross talk in the development of Reye's syndrome and suggest new therapeutic strategies for the prevention of hepatotoxicity associated with viral infections.

Our results also demonstrate that viral infections can alter the clearance of endogenous toxins that accumulate during normal metabolism. LCA, a secondary bile acid produced by intestinal bacteria, is metabolized by RXR heterodimers through the induction of cytochrome P450 family members such as CYP3A11, which catalyze the initial hydroxylation of LCA (67). Mice deficient in hepatocyte PXR or RXRα exhibit functional defects in the expression of LCA metabolic
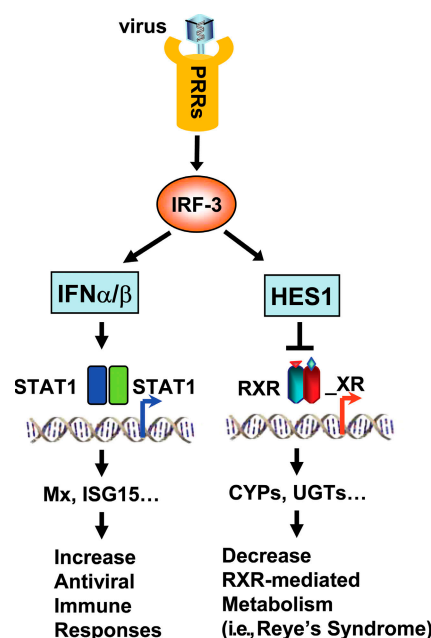
Figure 8. Model of IRF3 nuclear receptor cross talk and biological consequence. Activation of IRF3 through pattern recognition receptors (PRRs) results in the induction of antiviral genes through type I IFNs or the repression of RXRα target genes through Hes1. The repression of RXRα target genes, such as CYPs and UGTs, results in a decrease in RXR-mediated metabolism and pathogenesis of metabolic disorders such as Reye's syndrome.

genes (18, 27, 41). Excess amounts of LCA disturb liver homeostasis and result in cholestasis, which can be alleviated by the activation of PXR/RXR with less toxic but more potent nuclear receptor agonists such as PCN (18, 27). In this work, we have shown that activation of IRF3 during viral infection inhibits PXR/RXR-dependent activation of *CYP3A11.* Consequently, viral infections render mice highly susceptible to LCA-mediated cholestasis and hepatotoxicity. Interestingly, this mechanism may be relevant to viral-induced cholestasis in humans, as Epstein-Barr virus infections have been linked to cholestasis (68). The molecular pathways elucidated in our study will likely provide a useful framework for further investigation into this connection.

IRF3 is a transcription factor best known for its function in type I IFN production during the innate immune response against viral infections. Our experiments have identified a new function for virally activated IRF3, repression of $RXR\alpha$, that is independent of the type I IFN pathway. We have shown that activation of IRF3 induces expression of the transcriptional repressor Hes1, which binds directly to the proximal promoter of $RXR\alpha$ and recruits HDAC1 to repress transcription. Nevertheless, $RXR\alpha$ protein levels remain relatively stable in the absence of a nuclear receptor–activating signal. However, in combination with 26S proteosome complex activation by nuclear agonists (ASA, PCN, LG268, and GW3965), this pathway results in a biologically important loss of $RXR\alpha$ protein that would not be seen in the absence of IRF3 activation, where $RXR\alpha$ protein levels are replenished as new transcript is continually made. Although the repression of other nuclear receptors may contribute to our observed phenomenons, mutation of $RXR\alpha$ in hepatocytes results in similar in vivo defects in PXR/RXR target gene induction and increased LCA sensitivity, as seen in our experiments with polyI:C and VSV, providing further evidence that IRF3-mediated down-regulation of $RXR\alpha$ could contribute substantially to the pathogenesis of hepatic metabolic diseases (41). Previous work has shown that nuclear receptor activation can inhibit IRF3 target genes (39). It is possible that the down-regulation of $RXR\alpha$ may relieve this inhibitory effect and allow for optimal induction of IRF3 target genes involved in antiviral response. However, it is not clear whether this $RXR\alpha$ down-regulation will be beneficial overall or harmful to the host during a microbial infection.

The central role of $RXR\alpha$ in nuclear receptor signaling raises the possibility that IRF3–nuclear receptor cross talk may have implications for a variety of pathways and metabolic functions. The particular importance of the $RXR\alpha$ isoform is clear in that $RXR\alpha$-deficient mice are embryonic lethal (19, 69). Furthermore, several tissue-specific $RXR\alpha$-deficient mice have been described that point to diverse functions for this receptor (26, 40, 41). Loss of $RXR\alpha$ has been demonstrated in our work and by others to inhibit some, but not all, RXR heterodimer target genes, suggesting that other factors may play overlapping roles in determining activation and maintenance of certain nuclear receptor target genes (31, 41). However, it is clear from our work and these genetic studies of $RXR\alpha$ that loss of $RXR\alpha$ would affect several nuclear receptor pathways. Thus, in addition to contributing to the pathogenesis of Reye's syndrome, IRF3 repression of $RXR\alpha$ may contribute to other diseases associated with viral infections. One such disease is atherosclerosis, where IRF3 activation contributes to negative regulation of LXR–related genes and cholesterol efflux (31). It will be interesting to explore whether IRF3-dependent down-regulation of $RXR\alpha$ influences disorders such as Gianotti-Crosti syndrome in the skin (6, 70) and viral-linked diabetes (5). IRF3–nuclear receptor cross talk provides a new understanding of the link between microbial infection and metabolic dysfunction and suggests novel targets for therapeutic intervention in these syndromes.

MATERIALS AND METHODS

Cell culture and mice. Mouse BMMs were differentiated from marrow as described previously (71). IFNAR$^{-/-}$ and IRF3$^{-/-}$ mice (a gift from T. Taniguchi, University of Tokyo, Tokyo, Japan) were obtained as previously described (71). Cells from F5 C57BL/6 littermate wild-type mice were used as wild-type controls for experiments using cells from IFNAR$^{-/-}$ and IRF3$^{-/-}$ mice. C57BL/6 mice were used for all experiments not involving IFNAR$^{-/-}$ and IRF3$^{-/-}$ mice (obtained from Jackson ImmunoResearch Laboratories). RAW 264.7 mouse macrophage cells were cultured in DMEM supplemented with 10% fetal bovine serum and 1% penicillin/streptomycin. Stable RAW-RXRα or RAW-MT vector cells and Huh7-RXRα or Huh7-MT vector cells were made by retroviral transduction and selected with puromycin. Stable RAW-Hes1 or RAW-MT vector was made by transfecting RAW 264.7 cells with 5 μg pCMV-Hes1 or 5 μg pCMV and 0.5 μg pBabe-puro with Superfect (QIAGEN) and selected with puromycin.

Virus collection and quantification. GFP-tagged VSV was a kind gift from G. Barber (University of Miami, Miami, FL). The virus was grown on nearly confluent Madin Darby canine kidney (MDCK) cells, infected at a multiplicity of infection of 0.001. 2 d after infection, cell-free supernatant was ultracentrifuged at >100,000 *g* through a 25% sucrose cushion. The viral pellet was resuspended in PBS. Standard plaque assay was used to determine the number of PFU. In brief, confluent monolayers of MDCK cells in 6- or 12-well plates were infected in duplicate with serial dilution of the viral stock with intermittent shaking for 1 h. Subsequently, cells were overlaid with 1× MEM BSA containing 0.7% low-melting-point agar. Plaques were allowed to develop over 24–36 h and counted after staining cells with crystal violet.

Reagents. Specific pattern recognition receptor activation was achieved using polyI:C for TLR3/retinoic acid–inducible gene I (GE Healthcare) and *Escherichia coli* LPS for TLR4 (Sigma-Aldrich). Synthetic nuclear receptor ligands (a gift from T. Willson, GlaxoSmithKline, Research Triangle Park, NC) were obtained as previously described (31). LCA, PCN, and ASA were obtained from Sigma-Aldrich. 1,25(OH)$_2$D$_3$ was obtained from BIOMOL Research Laboratories, Inc. Rifampicin was obtained from Calbiochem. Actinomycin D and TSA were obtained from Sigma-Aldrich. Macrophage-CSF–containing media was obtained by growing L929 cells 4 d past confluency and harvesting the conditioned media.

Animal treatments. Age-matched 8–10-wk-old mice were used for all experiments. For hepatic nuclear receptor activation and liver functions analysis, mice were given vehicle (1% DMSO, maize oil), 75 mg/kg PCN, and 7.5 mg/kg 1,25(OH)$_2$D$_3$ by gavage and/or 0.25 mg/kg LCA i.p. for 4 d. For polyI:C experiments, mice were also treated with 0.1% NaCl or 150 μg polyI:C i.v. on day 1 or 3. For viral infection studies, mice were treated with 0.1% NaCl or 2.5×10^7 PFU VSV i.v. on day 1. On day 5, mice were

killed, and serum and liver samples were collected. ASA treatment was done as previously described (72). ASA treatment was done for 3–4 d. Serum ALT (TECO Diagnostics), serum ammonia (Pointe Scientific), blood glucose (LifeScan), and total serum bilirubin (Wako) levels were determined using the manufacturers' protocols. p-values were determined by independent *t* tests compared with controls, unless indicate otherwise in the figure legends. Animal studies were done in accordance with the Animal Research Committee of the University of California, Los Angeles.

RNA quantitation. For Q-PCR, total RNA was isolated, and cDNA was synthesized as described previously (71). PCR was then performed using the thermocycler (iCycler; Bio-Rad Laboratories). Q-PCR was conducted in a final volume of 25 µl containing: Taq polymerase, 1× Taq buffer (Stratagene), 125 µM deoxyribonucleoside triphosphate, SYBR green I (Invitrogen), and fluoroscein (Bio-Rad Laboratories), using oligo-dT cDNA or random hexamer cDNA as the PCR template. Amplification conditions were 95°C (3 min) and 40 cycles of 95°C (20 s), 55°C (30 s), and 72°C (20 s).

Western blot protein analysis. For Western blots, cell lysates were incubated at room temperature for 5 min with EB lysis buffer (10 mM Tris-HCl buffer, pH 7.4, containing 5 mM EDTA, 50 mM NaCl, 0.1% (wt/vol) BSA, 1% (vol/vol) Triton X-100, and protease inhibitors), size-separated in 10% SDS-PAGE, and transferred to nitrocellulose. RXRα and USF2 protein levels were detected using rabbit anti-RXRα or anti-USF2 antibody (Santa Cruz Biotechnology, Inc.). Whole-cell extract from livers were isolated as follows: livers were briefly homogenized in 1× PBS/protease inhibitors, the homogenized product was centrifuged, and the pellet was incubated at room temperature for 5 min with EB buffer.

Chromatin immunoprecipitation. CYP3A4 chromatin immunoprecipitation was done as previously described (73). For RXRα chromatin immunoprecipitation, inactivated and activated cells were fixed at room temperature for 10 min by adding formaldehyde directly to the culture medium to a final concentration of 1%. The reaction was stopped by adding glycine at a final concentration of 0.125 M for 5 min at room temperature. After three ice-cold PBS washes, the cells were collected and lysed for 10 min on ice in cell lysis buffer (5 mM PIPES [piperazine-N,N′-bis(2-ethane-sulfonic acid)], pH 8, 85 mM KCl, 0.5% NP-40, and protease inhibitors). The nuclei were resuspended in nuclei lysis buffer (50 mM Tris-HCl, pH 8.1, 10 mM EDTA, 1% SDS, and protease inhibitors) and incubated on ice for 10 min. Chromatin was sheared into 500- to 1,000-bp fragments by sonication and was precleared with protein A or protein G–Sepharose beads. The purified chromatin was diluted with chromatin immunoprecipitation dilution buffer (0.01% SDS, 1.1% Triton X-100, 1.2 mM EDTA, 16.7 mM Tris-HCl, pH 8.1, 167 mM NaCl, and protease inhibitors) and immunoprecipitated overnight at 4°C using 2–4 µg of anti-Hes1 (Santa Cruz Biotechnology, Inc.) or anti-HDAC1 (Upstate Biotechnology). Immune complexes were collected with protein G–Sepharose beads, washed thoroughly, and eluted. After protein-DNA cross-linking was reversed and the DNA was purified, the presence of selected DNA sequences was assessed by PCR. PCR products were analyzed on a 2% agarose gel and quantified with ImageJ (W.S. Rasband, National Institutes of Health, Bethesda, MD; http://rsb.info.nih.gov/ij/index.html).

siRNA assays. Targeted sequences for the Hes1 siRNA duplex or nonspecific siRNA duplex were synthesized by Invitrogen. Duplex oligonucleotides were transfected using Lipofectamine (Invitrogen) at a ratio of 10–20 pmol of RNA to 1.5 µl of Lipofectamine in serum-free, antibiotic-free media. Media was changed after 4–6 h, and experiments were done 36 h after transfection. The target sequence for the Hes1 siRNA was 5′-CGACACC-GGACAAACCAAA-3′ (74). The target sequence for the RXRα siRNA was 5′-AAGCACUAUGGAGUGUACAGC-3′ (75).

Histology. For hematoxylin and eosin (H&E) staining, liver samples were fixed in formalin for 48 h. H&E stainings were done by the University of

California, Los Angeles Tissue Procurement Core Laboratory (TPCL). For oil red O staining, liver samples were snap frozen in OCT compound (Sakura Finetek), and frozen tissue sections were made by TPCL. Oil red O staining was done in accordance with manufacturer's protocol (Diagnostic BioSystems). In brief, slides were placed in propylene glycol for 2 min, followed by oil red O staining for 6 min at 60°C. Slides were washed, and tissue was differentiated in 85% propylene glycol for 1 min, followed by modified Mayer's hematoxylin staining for 1 min. Slides were again extensively washed, and a coverslip was added with an aqueous mounting medium.

Online supplemental material. Fig. S1 shows repression of hepatic nuclear receptor target genes by polyI:C/VSV. Fig. S2 shows RXRα expression levels by Western blot in RXRα-expressing cell lines, compared with their controls. Fig. S3 depicts polyI:C repression of PCN–induced *UGT1A6* mRNA and ASA induction of PXR/RXR target genes. Fig. S4 depicts polyI:C potentiation of ASA-induced mitochondrial damage. Figs. S1–S4 are available at http://www.jem.org/cgi/content/full/jem.20060929/DC1.

REFERENCES

1. Alber, D.G., K.L. Powell, P. Vallance, D.A. Goodwin, and C. Grahame-Clarke. 2000. Herpesvirus infection accelerates atherosclerosis in the apolipoprotein E-deficient mouse. *Circulation*. 102:779–785.

2. Ruben, F.L., E.J. Streiff, M. Neal, and R.H. Michaels. 1976. Epidemiologic studies of Reye's syndrome: cases seen in Pittsburgh, October 1973-April 1975. *Am. J. Public Health*. 66:1096–1098.

3. Mondy, K., and P. Tebas. 2003. Emerging bone problems in patients infected with human immunodeficiency virus. *Clin. Infect. Dis.* 36: S101–S105.

4. Shaker, J.L., W.R. Reinus, and M.P. Whyte. 1998. Hepatitis C-associated osteosclerosis: late onset after blood transfusion in an elderly woman. *J. Clin. Endocrinol. Metab.* 83:93–98.

5. Ratziu, V., A. Heurtier, L. Bonyhay, T. Poynard, and P. Giral. 2005. Review article: an unexpected virus–host interaction – the hepatitis C virus-diabetes link. *Aliment. Pharmacol. Ther.* 22:56–60.

6. Michitaka, K., N. Horiike, Y. Chen, T.N. Duong, I. Konishi, T. Mashiba, Y. Tokumoto, Y. Hiasa, Y. Tanaka, M. Mizokami, and M. Onji. 2004. Gianotti-Crosti syndrome caused by acute hepatitis B virus genotype D infection. *Intern. Med.* 43:696–699.

7. Shi, L., N. Tu, and P.H. Patterson. 2005. Maternal influenza infection is likely to alter fetal brain development indirectly: the virus is not detected in the fetus. *Int. J. Dev. Neurosci.* 23:299–305.

8. Carlberg, C., I. Bendik, A. Wyss, E. Meier, L.J. Sturzenbecker, J.F. Grippo, and W. Hunziker. 1993. Two nuclear signalling pathways for vitamin D. *Nature*. 361:657–660.

9. Leid, M., P. Kastner, R. Lyons, H. Nakshatri, M. Saunders, T. Zacharewski, J.Y. Chen, A. Staub, J.M. Garnier, S. Mader, et al. 1992. Purification, cloning, and RXR identity of the HeLa cell factor with which RAR or TR heterodimerizes to bind target sequences efficiently. *Cell*. 68:377–395.

10. Pascussi, J.M., Y. Jounaidi, L. Drocourt, J. Domergue, C. Balabaud, P. Maurel, and M.J. Vilarem. 1999. Evidence for the presence of a functional pregnane X receptor response element in the CYP3A7 promoter gene. *Biochem. Biophys. Res. Commun.* 260:377–381.

11. Tontonoz, P., E. Hu, and B.M. Spiegelman. 1994. Stimulation of adipogenesis in fibroblasts by PPAR gamma 2, a lipid-activated transcription factor. *Cell*. 79:1147–1156.

12. Tontonoz, P., E. Hu, R.A. Graves, A.I. Budavari, and B.M. Spiegelman. 1994. mPPAR gamma 2: tissue-specific regulator of an adipocyte enhancer. *Genes Dev.* 8:1224–1234.

13. Willy, P.J., K. Umesono, E.S. Ong, R.M. Evans, R.A. Heyman, and D.J. Mangelsdorf. 1995. LXR, a nuclear receptor that defines a distinct retinoid response pathway. *Genes Dev.* 9:1033–1045.

14. Honkakoski, P., I. Zelko, T. Sueyoshi, and M. Negishi. 1998. The nuclear orphan receptor CAR-retinoid X receptor heterodimer activates the phenobarbital-responsive enhancer module of the CYP2B gene. *Mol. Cell. Biol.* 18:5652–5658.

15. Laffitte, B.A., H.R. Kast, C.M. Nguyen, A.M. Zavacki, D.D. Moore, and P.A. Edwards. 2000. Identification of the DNA binding specificity and potential target genes for the farnesoid X-activated receptor. *J. Biol. Chem.* 275:10638–10647.

16. Issemann, I., R.A. Prince, J.D. Tugwood, and S. Green. 1993. The retinoid X receptor enhances the function of the peroxisome proliferator activated receptor. *Biochimie.* 75:251–256.

17. Gearing, K.L., M. Gottlicher, M. Teboul, E. Widmark, and J.A. Gustafsson. 1993. Interaction of the peroxisome-proliferator-activated receptor and retinoid X receptor. *Proc. Natl. Acad. Sci. USA.* 90:1440–1444.

18. Xie, W., A. Radominska-Pandya, Y. Shi, C.M. Simon, M.C. Nelson, E.S. Ong, D.J. Waxman, and R.M. Evans. 2001. An essential role for nuclear receptors SXR/PXR in detoxification of cholestatic bile acids. *Proc. Natl. Acad. Sci. USA.* 98:3375–3380.

19. Sucov, H.M., E. Dyson, C.L. Gumeringer, J. Price, K.R. Chien, and R.M. Evans. 1994. RXR alpha mutant mice establish a genetic basis for vitamin A signaling in heart morphogenesis. *Genes Dev.* 8:1007–1018.

20. Janowski, B.A., P.J. Willy, T.R. Devi, J.R. Falck, and D.J. Mangelsdorf. 1996. An oxysterol signalling pathway mediated by the nuclear receptor LXR alpha. *Nature.* 383:728–731.

21. Kliewer, S.A., J.T. Moore, L. Wade, J.L. Staudinger, M.A. Watson, S.A. Jones, D.D. McKee, B.B. Oliver, T.M. Willson, R.H. Zetterstrom, et al. 1998. An orphan nuclear receptor activated by pregnanes defines a novel steroid signaling pathway. *Cell.* 92:73–82.

22. Sakashita, A., M. Kizaki, S. Pakkala, G. Schiller, N. Tsuruoka, R. Tomosaki, J.F. Cameron, M.I. Dawson, and H.P. Koeffler. 1993. 9-cis-retinoic acid: effects on normal and leukemic hematopoiesis in vitro. *Blood.* 81:1009–1016.

23. Wu, Y., X. Zhang, F. Bardag-Gorce, R.C. Robel, J. Aguilo, L. Chen, Y. Zeng, K. Hwang, S.W. French, S.C. Lu, and Y.J. Wan. 2004. Retinoid X receptor alpha regulates glutathione homeostasis and xenobiotic detoxification processes in mouse liver. *Mol. Pharmacol.* 65:550–557.

24. Makishima, M., A.Y. Okamoto, J.J. Repa, H. Tu, R.M. Learned, A. Luk, M.V. Hull, K.D. Lustig, D.J. Mangelsdorf, and B. Shan. 1999. Identification of a nuclear receptor for bile acids. *Science.* 284:1362–1365.

25. Makishima, M., T.T. Lu, W. Xie, G.K. Whitfield, H. Domoto, R.M. Evans, M.R. Haussler, and D.J. Mangelsdorf. 2002. Vitamin D receptor as an intestinal bile acid sensor. *Science.* 296:1313–1316.

26. Imai, T., M. Jiang, P. Chambon, and D. Metzger. 2001. Impaired adipogenesis and lipolysis in the mouse upon selective ablation of the retinoid X receptor alpha mediated by a tamoxifen-inducible chimeric Cre recombinase (Cre-ERT2) in adipocytes. *Proc. Natl. Acad. Sci. USA.* 98:224–228.

27. Staudinger, J.L., B. Goodwin, S.A. Jones, D. Hawkins-Brown, K.I. MacKenzie, A. LaTour, Y. Liu, C.D. Klaassen, K.K. Brown, J. Reinhard, et al. 2001. The nuclear receptor PXR is a lithocholic acid sensor that protects against liver toxicity. *Proc. Natl. Acad. Sci. USA.* 98:3369–3374.

28. Beigneux, A.P., A.H. Moser, J.K. Shigenaga, C. Grunfeld, and K.R. Feingold. 2000. The acute phase response is associated with retinoid X receptor repression in rodent liver. *J. Biol. Chem.* 275:16390–16399.

29. Beigneux, A.P., A.H. Moser, J.K. Shigenaga, C. Grunfeld, and K.R. Feingold. 2002. Reduction in cytochrome P-450 enzyme expression is associated with repression of CAR (constitutive androstane receptor) and PXR (pregnane X receptor) in mouse liver during the acute phase response. *Biochem. Biophys. Res. Commun.* 293:145–149.

30. Kim, M.S., J. Shigenaga, A. Moser, K. Feingold, and C. Grunfeld. 2003. Repression of farnesoid X receptor during the acute phase response. *J. Biol. Chem.* 278:8988–8995.

31. Castrillo, A., S.B. Joseph, S.A. Vaidya, M. Haberland, A.M. Fogelman, G. Cheng, and P. Tontonoz. 2003. Crosstalk between LXR and toll-like receptor signaling mediates bacterial and viral antagonism of cholesterol metabolism. *Mol. Cell.* 12:805–816.

32. Perry, A.K., E.K. Chow, J.B. Goodnough, W.C. Yeh, and G. Cheng. 2004. Differential requirement for TANK-binding kinase–1 in type I interferon responses to Toll-like receptor activation and viral infection. *J. Exp. Med.* 199:1651–1658.

33. Yamamoto, M., S. Sato, H. Hemmi, K. Hoshino, T. Kaisho, H. Sanjo, O. Takeuchi, M. Sugiyama, M. Okabe, K. Takeda, and S. Akira. 2003. Role of adaptor TRIF in the MyD88-independent toll-like receptor signaling pathway. *Science.* 301:640–643.

34. Li, K., Z. Chen, N. Kato, M. Gale Jr., and S.M. Lemon. 2005. Distinct poly(I-C) and virus-activated signaling pathways leading to interferon-beta production in hepatocytes. *J. Biol. Chem.* 280:16739–16747.

35. Yoneyama, M., M. Kikuchi, T. Natsukawa, N. Shinobu, T. Imaizumi, M. Miyagishi, K. Taira, S. Akira, and T. Fujita. 2004. The RNA helicase RIG-I has an essential function in double-stranded RNA-induced innate antiviral responses. *Nat. Immunol.* 5:730–737.

36. Fitzgerald, K.A., D.C. Rowe, B.J. Barnes, D.R. Caffrey, A. Visintin, E. Latz, B. Monks, P.M. Pitha, and D.T. Golenbock. 2003. LPS-TLR4 signaling to IRF-3/7 and NF-κB involves the Toll adapters TRAM and TRIF. *J. Exp. Med.* 198:1043–1055.

37. Jiang, Z., T.W. Mak, G. Sen, and X. Li. 2004. Toll-like receptor 3-mediated activation of NF-kappaB and IRF3 diverges at Toll-IL-1 receptor domain-containing adapter inducing IFN-beta. *Proc. Natl. Acad. Sci. USA.* 101:3533–3538.

38. Leung, T.H., A. Hoffmann, and D. Baltimore. 2004. One nucleotide in a kappaB site can determine cofactor specificity for NF-kappaB dimers. *Cell.* 118:453–464.

39. Ogawa, S., J. Lozach, C. Benner, G. Pascual, R.K. Tangirala, S. Westin, A. Hoffmann, S. Subramaniam, M. David, M.G. Rosenfeld, and C.K. Glass. 2005. Molecular determinants of crosstalk between nuclear receptors and toll-like receptors. *Cell.* 122:707–721.

40. Li, M., A.K. Indra, X. Warot, J. Brocard, N. Messaddeq, S. Kato, D. Metzger, and P. Chambon. 2000. Skin abnormalities generated by temporally controlled RXRalpha mutations in mouse epidermis. *Nature.* 407:633–636.

41. Wan, Y.J., D. An, Y. Cai, J.J. Repa, T. Hung-Po Chen, M. Flores, C. Postic, M.A. Magnuson, J. Chen, K.R. Chien, et al. 2000. Hepatocyte-specific mutation establishes retinoid X receptor alpha as a heterodimeric integrator of multiple physiological processes in the liver. *Mol. Cell. Biol.* 20:4436–4444.

42. Gianni, M., A. Bauer, E. Garattini, P. Chambon, and C. Rochette-Egly. 2002. Phosphorylation by p38MAPK and recruitment of SUG-1 are required for RA-induced RAR gamma degradation and transactivation. *EMBO J.* 21:3760–3769.

43. Porsch-Ozcurumez, M., T. Langmann, S. Heimerl, H. Borsukova, W.E. Kaminski, W. Drobnik, C. Honer, C. Schumacher, and G. Schmitz. 2001. The zinc finger protein 202 (ZNF202) is a transcriptional repressor of ATP binding cassette transporter A1 (ABCA1) and ABCG1 gene expression and a modulator of cellular lipid efflux. *J. Biol. Chem.* 276:12427–12433.

44. Steffensen, K.R., E. Holter, N. Alikhani, W. Eskild, and J.A. Gustafsson. 2003. Glucocorticoid response and promoter occupancy of the mouse LXRalpha gene. *Biochem. Biophys. Res. Commun.* 312:716–724.

45. Aguilera, C., R. Hoya-Arias, G. Haegeman, L. Espinosa, and A. Bigas. 2004. Recruitment of IkappaBalpha to the hes1 promoter is associated with transcriptional repression. *Proc. Natl. Acad. Sci. USA.* 101:16537–16542.

46. Nuthall, H.N., J. Husain, K.W. McLarren, and S. Stifani. 2002. Role for Hes1-induced phosphorylation in Groucho-mediated transcriptional repression. *Mol. Cell. Biol.* 22:389–399.

47. Ciotti, M., A. Marrone, C. Potter, and I.S. Owens. 1997. Genetic polymorphism in the human UGT1A6 (planar phenol) UDP-glucuronosyltransferase: pharmacological implications. *Pharmacogenetics.* 7:485–495.

48. Vyhlidal, C.A., P.K. Rogan, and J.S. Leeder. 2004. Development and refinement of pregnane X receptor (PXR) DNA binding site model

using information theory: insights into PXR–mediated gene regulation. *J. Biol. Chem.* 279:46779–46786.

49. Belay, E.D., J.S. Bresee, R.C. Holman, A.S. Khan, A. Shahriari, and L.B. Schonberger. 1999. Reye's syndrome in the United States from 1981 through 1997. *N. Engl. J. Med.* 340:1377–1382.

50. Mitchell, R.A., J.S. Partin, E.L. Arcinue, J.C. Partin, M.L. Ram, and A.P. Sarnaik. 1985. Prognosis and diagnosis of Reye syndrome by discriminant analysis. *Exp. Mol. Pathol.* 43:268–273.

51. Davis, L.E., B.M. Woodfin, T.Q. Tran, L.S. Caskey, J.M. Wallace, O.U. Scremin, and K.S. Blisard. 1993. The influenza B virus mouse model of Reye's syndrome: pathogenesis of the hypoglycaemia. *Int. J. Exp. Pathol.* 74:251–258.

52. Dolphin, C.T., J. Caldwell, and R.L. Smith. 1987. Effect of interferon synthesis upon the metabolism of [carboxyl-14C]-aspirin in the mouse. *Biochem. Pharmacol.* 36:2437–2442.

53. Dupont, I., F. Berthou, P. Bodenez, L. Bardou, C. Guirriec, N. Stephan, Y. Dreano, and D. Lucas. 1999. Involvement of cytochromes P-450 2E1 and 3A4 in the 5-hydroxylation of salicylate in humans. *Drug Metab. Dispos.* 27:322–326.

54. Lindell, M., M.O. Karlsson, H. Lennernas, L. Pahlman, and M.A. Lang. 2003. Variable expression of CYP and Pgp genes in the human small intestine. *Eur. J. Clin. Invest.* 33:493–499.

55. Kuehl, G.E., J. Bigler, J.D. Potter, and J.W. Lampe. 2006. Glucuronidation of the aspirin metabolite salicylic acid by expressed UDP-glucuronosyltransferases and human liver microsomes. *Drug Metab. Dispos.* 34:199–202.

56. Trost, L.C., and J.J. Lemasters. 1997. Role of the mitochondrial permeability transition in salicylate toxicity to cultured rat hepatocytes: implications for the pathogenesis of Reye's syndrome. *Toxicol. Appl. Pharmacol.* 147:431–441.

57. Pronicka, E. 1999. Reye's syndrome—diagnostic challenge. [In Polish.] *Pediatr. Pol.* 74:107–110.

58. Iwanczak, F., J. Prandota, and Z. Smykowa. 1973. Two cases of Stevens-Johnson syndrome in children. [In Polish.] *Wiad. Lek.* 26:1539–1542.

59. Reye, R.D., G. Morgan, and J. Baral. 1963. Encephalopathy and fatty degeneration of the viscera. A disease entity in childhood. *Lancet.* 91:749–752.

60. Duerksen, D.R., L.D. Jewell, A.L. Mason, and V.G. Bain. 1997. Co-existence of hepatitis A and adult Reye's syndrome. *Gut.* 41:121–124.

61. Orlowski, J.P., P. Campbell, and S. Goldstein. 1990. Reye's syndrome: a case control study of medication use and associated viruses in Australia. *Cleve. Clin. J. Med.* 57:323–329.

62. Ghosh, D., D. Dhadwal, A. Aggarwal, S. Mitra, S.K. Garg, R. Kumar, and B. Kaur. 1999. Investigation of an epidemic of Reye's syndrome in northern region of India. *Indian Pediatr.* 36:1097–1106.

63. Treon, S.P., and S.A. Broitman. 1992. Monoclonal antibody therapy in the treatment of Reye's syndrome. *Med. Hypotheses.* 39:238–242.

64. Partin, J.C., W.K. Schubert, and J.S. Partin. 1971. Mitochondrial ultrastructure in Reye's syndrome (encephalopathy and fatty degeneration of the viscera). *N. Engl. J. Med.* 285:1339–1343.

65. Martens, M.E., C.H. Chang, and C.P. Lee. 1986. Reye's syndrome: mitochondrial swelling and Ca2+ release induced by Reye's plasma, allantoin, and salicylate. *Arch. Biochem. Biophys.* 244:773–786.

66. Tomoda, T., K. Takeda, T. Kurashige, H. Enzan, and M. Miyahara. 1994. Acetylsalicylate (ASA)-induced mitochondrial dysfunction and its potentiation by Ca2+. *Liver.* 14:103–108.

67. Araya, Z., and K. Wikvall. 1999. 6alpha-hydroxylation of taurochenodeoxycholic acid and lithocholic acid by CYP3A4 in human liver microsomes. *Biochim. Biophys. Acta.* 1438:47–54.

68. Shaukat, A., H.T. Tsai, R. Rutherford, and F.A. Anania. 2005. Epstein-Barr virus induced hepatitis: an important cause of cholestasis. *Hepatol. Res.* 33:24–26.

69. Kastner, P., J.M. Grondona, M. Mark, A. Gansmuller, M. LeMeur, D. Decimo, J.L. Vonesch, P. Dolle, and P. Chambon. 1994. Genetic analysis of RXR alpha developmental function: convergence of RXR and RAR signaling pathways in heart and eye morphogenesis. *Cell.* 78:987–1003.

70. Yoshida, M., N. Tsuda, T. Morihata, H. Sugino, and T. Iizuka. 2004. Five patients with localized facial eruptions associated with Gianotti-Crosti syndrome caused by primary Epstein-Barr virus infection. *J. Pediatr.* 145:843–844.

71. Doyle, S., S. Vaidya, R. O'Connell, H. Dadgostar, P. Dempsey, T. Wu, G. Rao, R. Sun, M. Haberland, R. Modlin, and G. Cheng. 2002. IRF3 mediates a TLR3/TLR4-specific antiviral gene program. *Immunity.* 17:251–263.

72. Paul, A., L. Calleja, J. Camps, J. Osada, E. Vilella, N. Ferre, E. Mayayo, and J. Joven. 2000. The continuous administration of aspirin attenuates atherosclerosis in apolipoprotein E-deficient mice. *Life Sci.* 68:457–465.

73. Frank, C., H. Makkonen, T.W. Dunlop, M. Matilainen, S. Vaisanen, and C. Carlberg. 2005. Identification of pregnane X receptor binding sites in the regulatory regions of genes involved in bile acid homeostasis. *J. Mol. Biol.* 346:505–519.

74. Ross, D.A., P.K. Rao, and T. Kadesch. 2004. Dual roles for the Notch target gene Hes-1 in the differentiation of 3T3-L1 preadipocytes. *Mol. Cell. Biol.* 24:3505–3513.

75. Cao, X., W. Liu, F. Lin, H. Li, S.K. Kolluri, B. Lin, Y.H. Han, M.I. Dawson, and X.K. Zhang. 2004. Retinoid X receptor regulates Nur77/TR3-dependent apoptosis [corrected] by modulating its nuclear export and mitochondrial targeting. *Mol. Cell. Biol.* 24:9705–9725.